DSN–MVM'73 S/X Dual-Frequency Doppler Demonstration

F. B. Winn, K. W. Yip, and S. J. Reinbold
Tracking and Orbit Determination Section

Doppler charged-particle calibrations derived from S/X dual doppler data have been demonstrated successfully. The accuracy of the S/X dual doppler has been verified by comparisons to Faraday polarization data. This verification, limited by the accuracy of "mapped" Faraday data, is to the 10- to 30-cm level. The S/X dual doppler exhibits subcentimeter resolution and, thus, its potential accuracy. The S/X dual doppler calibrations are significant to the Mariner 10–Mercury encounter orbit determination. The error of the estimate of the Mariner 10–Mercury target plane coordinate was reduced by ~500 km (~80% improvement).

I. Introduction

The DSN successfully used the Mariner Venus/Mercury 1973 (MVM'73) mission (Mariner 10) to demonstrate that dual-frequency doppler measurements, when differenced, provide line-of-sight, radio metric doppler calibrations for charged-particle influences. These calibrations assess collectively the influences of the space plasma and Earth's ionosphere. Thus, when the plasma electron content variations are insignificant, the dual-frequency doppler data compare quite well with Faraday polarization data. In these instances, both measure variations in the Earth's ionospheric electron content.

The dual-frequency doppler was used to significantly improve the Mercury target plane position determinations based on the tracking data acquired from the one tracking station with a dual-frequency capability—DSS 14. The Mariner 10 position estimate error was reduced by ~80% (~500 km).

II. S/X Dual Doppler Quality (Verification)

A 2200-MHz (S-band) radio wave is transmitted from a DSS to the Mariner 10 spacecraft. The received frequency is then retransmitted at an S-band frequency 240/221 times higher. Simultaneously, the received frequency is also retransmitted at an X-band frequency. This transmitted X-band frequency is equal to the spacecraft received frequency multiplied by 880/221. The S- and X-band transmissions from the spacecraft are then received at DSS 14, which has the only dual-frequency receiver currently existing within the DSN. S/X dual Doppler exploits the inverse frequency squared dependence of the phase velocity change of a radio signal traversing a tenuous plasma. The doppler shifts present in the received S- and X-band tones measure two occurances: the radial motion of the spacecraft as seen from DSS 14, and the net change in the total number of electrons encountered along the ray path. That portion of the doppler shift resulting from radial motion of the

probe is removed by differencing the doppler shifts, and the balance is due to charged particle effects. In equation form, the procedure to compute the balance is

$$\text{Balance} = K(S - \frac{3}{11}X)/f_{q_s}$$

In other words, the X-band frequency is multiplied down to an equivalent S-band frequency and differenced from the S-band received frequency. This difference in the net frequency change at S-band is then due entirely to electron content variations. The ratio of the S-band frequency change to the S-band frequency can be easily converted to electron content variations or apparent range change of the spacecraft. (A detailed discussion of this physical process and the specific equations used are presented in the preceding article of this volume by G. A. Madrid, "The Measurement of Dispersive Effects Using the Mariner 10 S- and X-band Spacecraft to Station Link.)

To date, only two charged-particle calibrators can achieve submeter level precision: S/X dual doppler and Faraday polarization data (Ref. 1). Other calibrators, differenced range versus integrated doppler (DRVID) (Ref. 2) and dual S/X range, provide charged-particle assessments to the precision of the DSN range data which is typically meters.

It should be noted that the Faraday rotation data are obtained from measurements to geostationary satellites. At the Goldstone DSN complex (site of DSS 12 and DSS 14), three Faraday polarimeters[1] continuously monitor the amount of rotation experienced by the plane polarized transmissions of the Applied Technology Satellites ATS-1 and ATS-5. These observations provide a measure of Earth's ionospheric electron content and its time-rate of change. The Faraday polarization data must be mapped from the DSS–satellite line-of-sight to a planetary spacecraft. This mapping technique is based on a mathematical model (Ref. 1), which is frequently inadequate at low topocentric elevation angles. Typically, the uncertainty of mapped Faraday for lines-of-sight taken above 30 deg elevation is $\sim$0.1 m (1 σ). For elevation angles below 30 deg, the uncertainty is 0.3 m (1 σ).

The situation can be stated thus: If the S/X dual doppler data and the "mapped" Faraday polarization data show the same electron content history, within the precision of the "mapped" Faraday data, no plasma activity of significance is assumed to exist and the S/X dual doppler data are valid; if the S/X doppler data cannot be favorably compared to the Faraday data, it is possible that the S/X dual doppler is "seeing" solar plasma activity. In short, the S/X dual doppler can be verified only if it compares to the mapped Faraday data on some occasions.

The Faraday polarization data used in these comparisons were sampled every 10 min. The S/X dual doppler, as processed, only provides ½ the high-frequency resolution inherent in the data. A subsequent analysis will address the high-frequency structure of both data types in more detail.

Space plasma activity was usually insignificant during the MVM'73 mission (December 15, 1973 to March 29, 1974), thus permitting favorable comparisons of Faraday and S/X doppler data. A detailed analysis of the first three S/X dual doppler passes is available in the Appendix. About 60% of the S/X data passes compare well with the "mapped" Faraday data. For the other 40%, it was known that, some of the time, the differences between the S/X dual doppler and the Faraday data had nothing to do with charged particles. On these occasions, the DSS 14 experimental dual-frequency receiver (especially developed and installed for this demonstration by G. Levy and others) was being tested in a nonstandard operating mode or some component of the R&D ground-based hardware was known to be malfunctioning. When the DSS 14 R&D hardware was in a standard operating mode and functioning, usually the dual doppler and the Faraday data agreed.

Comparisons of the available S/X dual doppler and "mapped" Faraday data through Mercury flyby (March 29, 1974) are shown in Fig. 1. As can be seen, for some passes (ten in number), the dual doppler and Faraday agree over the entire tracking pass, i.e., the two calibrations do not differ by more than 0.1 m in cumulative range error change. Some passes (twelve in number) show similar agreement for the two calibrations when the elevation angle associated with the S/X dual doppler observation is greater than 30 deg. There are still other passes (seven in number) for which the differences between the two calibrations are in excess of 1 m. The passes shown having this character are believed to be exhibiting real space plasma effects. The evidence in support of this conjecture comes in four parts:

(1) S/X dual doppler data detection of high plasma activity.

(2) The charged-particle detector aboard the spacecraft recorded high ion levels and fluctuations.

[1]One of the polarimeters is deployed and used by the Stanford Radio Science Laboratory under the direction of T. Howard, the MVM'73 Radio Science Team Leader.

(3) S-band radio metric doppler showed structure not related to the normal phenomena encountered.

(4) Earth's ionosphere, as measured by the Faraday polarization data, was excited. This excitement stems from the solar plasma interaction with the ionosphere. The ionosphere showed activity 2.5 times higher than the normal at times.

There are six additional passes of S/X dual doppler data which do not correlate with the "mapped" Faraday data, and there are other indications that the dual doppler are unreasonable. These passes are still undergoing investigation.

Table 1 tabulates 27 S/X dual doppler–Faraday comparisons. From this tabulation it is apparent that ~40% of the dual doppler sample agrees with the Faraday. Another ~40% of the passes shows agreement for all data acquired above 30-deg elevation. The remaining 20% of the sample exhibits space plasma effects.

Besides the gross structure of the S/X dual doppler, which contains the charged-particle information, the dual doppler shows a high-frequency noise. An examination of the high-frequency data noise of the December 15, 1973 pass reveals the resolution of the dual doppler calibration technique (Fig. 2). Figure 2 plots about a 1-h segment of the S/X doppler data. The plot provides a high-resolution view of these data. The S/X dual doppler was acquired at a rate of one point per minute. A parabola was fit to the data shown. The detrended residuals produced by the fit have a standard deviation of 0.76 cm. Thus, the S/X data of Day 349 have near centimeter resolution. This is the anticipated noise level.

III. MVM'73 Orbit Determination: Short Data Arc Analysis—A Problem

Mariner 10 arrived at Mercury on March 29, 1974. It was launched from Earth 5 mo earlier. The Mariner 10 spacecraft moved along transfer orbits that carried it from Earth to Venus and from Venus to Mercury (Fig. 3). The Earth–Venus, Venus–Mercury ballistic trajectories were altered by corrective maneuvers of the spacecraft rocket and by gas leaks developed on the spacecraft. In all, there were six instances when the spacecraft experienced "large" nongravitational accelerations:

(1) Earth launch (November 3, 1973).

(2) Trajectory correction maneuver 1 (TCM1) (November 13, 1973).

(3) TCM2 (January 21, 1974).

(4) Gas leak (January 28, 1974).

(5) Gas leak (February 10, 1974).

(6) TCM3 (March 16, 1974).

Figure 3 shows their locations along the trajectories.

An examination of the Faraday and S/X dual doppler data shows that plasma activity appears to be insignificant for the time periods following the first five events: Earth launch, TCM1, TCM2, the January 28 gas leak, and the February 10 gas leak. Faraday polarization data were used to remove the ionospheric charged-particle effects from the DSS 12 and DSS 14 tracking data acquired during these periods. The improvements realized in the encounter navigation are detailed in Refs. 4, 5, 6, and 7. DRVID, as well as Faraday, was used for calibration for the post-Earth launch data segment. The DRVID calibrations and their significance to navigation is the subject of Ref. 8.

After each nongravitational acceleration of the probe, it is desirable to estimate the new orbit of the spacecraft and determine how this orbit will carry the probe to the target planet. This was accomplished by S. J. Reinbold, C. S. Christensen, and G. E. Pease of the Navigation Team. Initial estimates of the new trajectory used four days of tracking data. Now it is known that short data arc solutions of this kind are prone to be sensitive to charged-particle influences, i.e., erroneous orbit solutions can result (Ref. 3). This is particularly true of the plasma activity which is unusually high.

Plasma ion levels and fluctuations during the week following TCM3 seriously degraded the Mercury approach navigation. The existence of plasma disturbances was ascertained by three direct measurements: S/X dual doppler measurements from DSS 14, DRVID measurements from DSS 43 and DSS 63, and ion detector measurements[2] on the spacecraft. There are two additional sources that indicate large plasma activity: the earth's ionosphere became most excited during this time, frequently being over 2.5 times more active than normal; the S-band doppler, the principle data type used to track the spacecraft and to navigate the spacecraft, showed a medium amplitude structure (~10 mHz amplitude) (Fig. 4) of a nonperiodic nature during the week.

The analysis by the Navigation Team on the doppler tracking data, corrupted by such plasma variations, provided Mercury encounter position estimates which were inconsistent. The Mercury encounter position estimates

[2]C. Yeates, Radio Science Team, private communication.

were scattered over 550 km (5 day arc). To circumvent the plasma degradation, a data editing process was conducted by R. E. Koch (Navigation Team) that eventually deleted ~50% of the doppler tracking data acquired by DSS 14, DSS 43, and DSS 63. Only after this editing did the Mercury encounter solutions become consistent and reasonable. Post-Mercury encounter knowledge reveals that the error was less than 40 km at Mercury.

The distribution of the S/X dual doppler tracking passes over the 9-day data arc is pictured in Figs. 5a and 5b.

IV. Elimination of Charged-Particle Effects by S/X Dual Doppler Calibration

The phase velocity change of doppler induced by charged-particle variations can be interpreted falsely as an apparent range change of the spacecraft. Figure 1 shows what the apparent range change is for specific times as measured by Faraday polarization data and S/X dual doppler. However, it is doppler, not range, that is to be calibrated for electron content variations. Thus, it is the time-rate-of-change of the apparent range that is required.

During the 9 days following trajectory correction maneuver 3 (TCM3), when known plasma activity was occurring, six tracking passes of S/X dual doppler were acquired at DSS 14. The doppler calibrations computed from this dual S/X data are pictured in Fig. 6, along with the corresponding Faraday-based doppler calibrations.

Each plot in this figure corresponds to a tracking pass. Two of the plots, namely that of March 18 and March 24, show the two calibrations in reasonably good agreement. Thus, little plasma activity is present during these two passes. The remaining four passes, however, reveal plasma activity.

Figure 7 shows the doppler residuals that result when the Mariner 10 orbit is adjusted in a least squares process which fits the doppler tracking data (119 doppler data points) and range tracking data (20 range data points). These residuals exhibit biases (March 20, March 23), and slopes (March 16, March 18, and March 24).

Figure 8 shows how the after-the-fit doppler residuals appear when the doppler tracking data are calibrated for charged-particle effects before least squares fitting. The residuals that involved S/X dual-frequency data calibrations (with the one exception of the March 16 pass) do not show biases or slopes. The quality of the Doppler fit is improved in terms of the sum of the squares of the doppler residuals. The unit standard deviation of the doppler residuals decreased by over 70%. When Faraday polarization data were used as the doppler calibration source, the standard deviation of the doppler residuals decreased by ~50%.

V. Significance of Calibration to MVM'73 Navigation at Mercury Encounter

When the MVM'73 Navigation Team used the tracking data (doppler and range from DSS 14, DSS 43, and DSS 63) that was acquired in the 9 days following TCM3 (March 16, 1974), the estimates of the Mariner 10–Mercury encounter coordinates scattered over 200 km. Valid predictions of the Mariner 10 encounter coordinates were obtained by rejecting much of the plasma-affected doppler data. This "predicted" position is shown in Fig. 9 along with the actual position known to be "true" from Mercury flyby data.

When the DSS 12 and DSS 14 doppler tracking data are used to estimate the encounter coordinates of Mariner 10 with and without Faraday calibrations, it is found that the calibrations reduced the error of the estimates by ~60% (~110-km displacement) (Fig. 9). When DSS 14 data are used to estimate the encounter coordinates with and without S/X dual doppler calibrations, it is found that the calibrations reduce the error of the estimates by ~80% (~500-km displacement) (Fig. 10). These two solutions did not support Mercury approach navigation—they were arrived at after Mercury encounter as a demonstration of navigation capability improvements.

Another estimate of the encounter coordinates was made with a combination of the Faraday and S/X dual doppler calibrations. If S/X dual doppler existed for a pass, it was used. If it was not available, the Faraday calibrations were used. The improvement realized by the joint use of the two calibration types is ~80% (180-km displacement) (Fig. 11).

Charged-particle calibrations used in this data arc reduction, and in other data arc reductions (Refs. 4, 5, 6, and 7) have consistently decreased the error of the encounter position estimates.

VI. Summary

The S/X dual doppler has measured space plasma and the Earth's ionospheric charged-particle variations. These measurements were used in support of MVM'73 mission navigation.

Table. 1. MVM'73: S/X data quality relative to Faraday

Month	Day of month																													
	1	2	3	4	5	6	7	8	9	10	11	12	13	14	15	16	17	18	19	20	21	22	23	24	25	26	27	28	29	30	31
Nov.																															
Dec.															1															2	
Jan.			1											1	1							2	3	3		2				1	
Feb.					2	2	2		2							1			2			3									
Mar.	1						2			2						3	3	1		3			3/1	1				2	2		
Apr.																															

S/X dual doppler populations:

Population 1. S/X dual doppler and Faraday rotation data agree (difference < 0.1 m).

Population 2. S/X dual doppler and Faraday agree at higher elevations (difference < 0.1 m above 30 deg). S/X dual doppler and Faraday differences < 0.3 m above 10-deg elevation.

Population 3. Partial agreement or no agreement.

Entries in table indicate quality of S/X dual doppler–Faraday data comparisons.

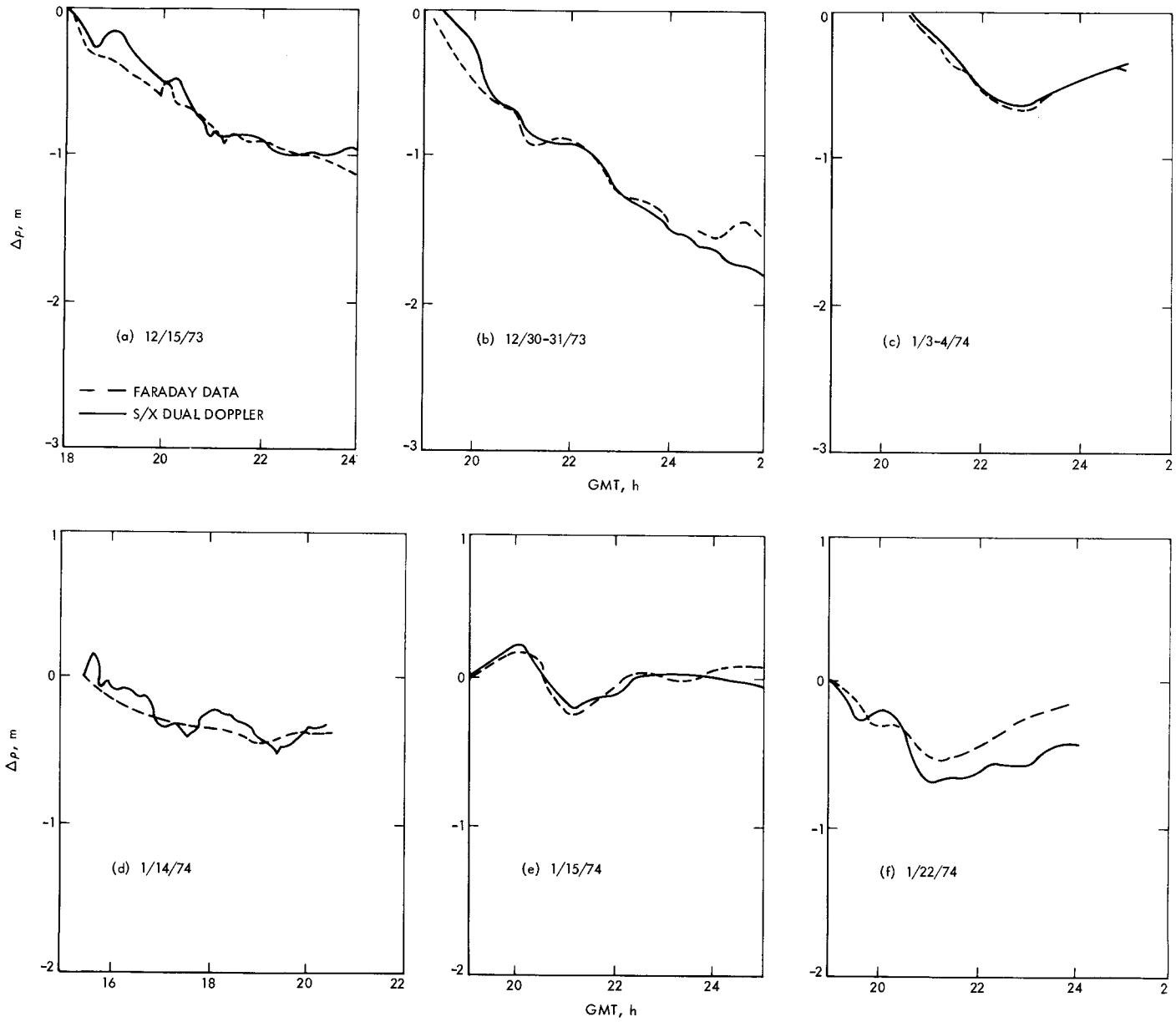

Fig. 1. S/X dual doppler and Faraday polarization data comparisons

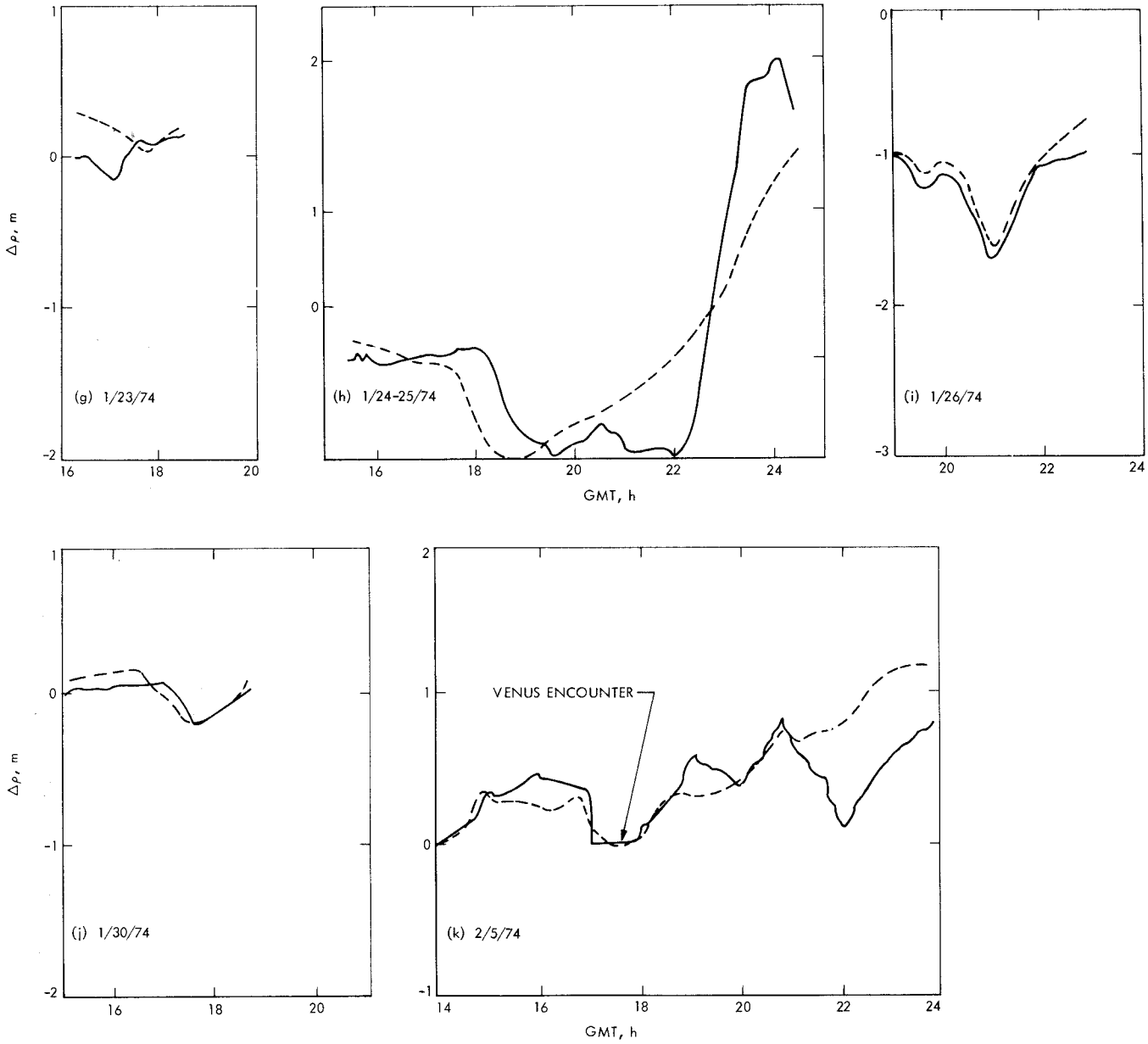
Δρ, m
(g) 1/23/74
(h) 1/24-25/74
(i) 1/26/74
GMT, h
(j) 1/30/74
VENUS ENCOUNTER
(k) 2/5/74
GMT, h

Fig. 1 (contd)

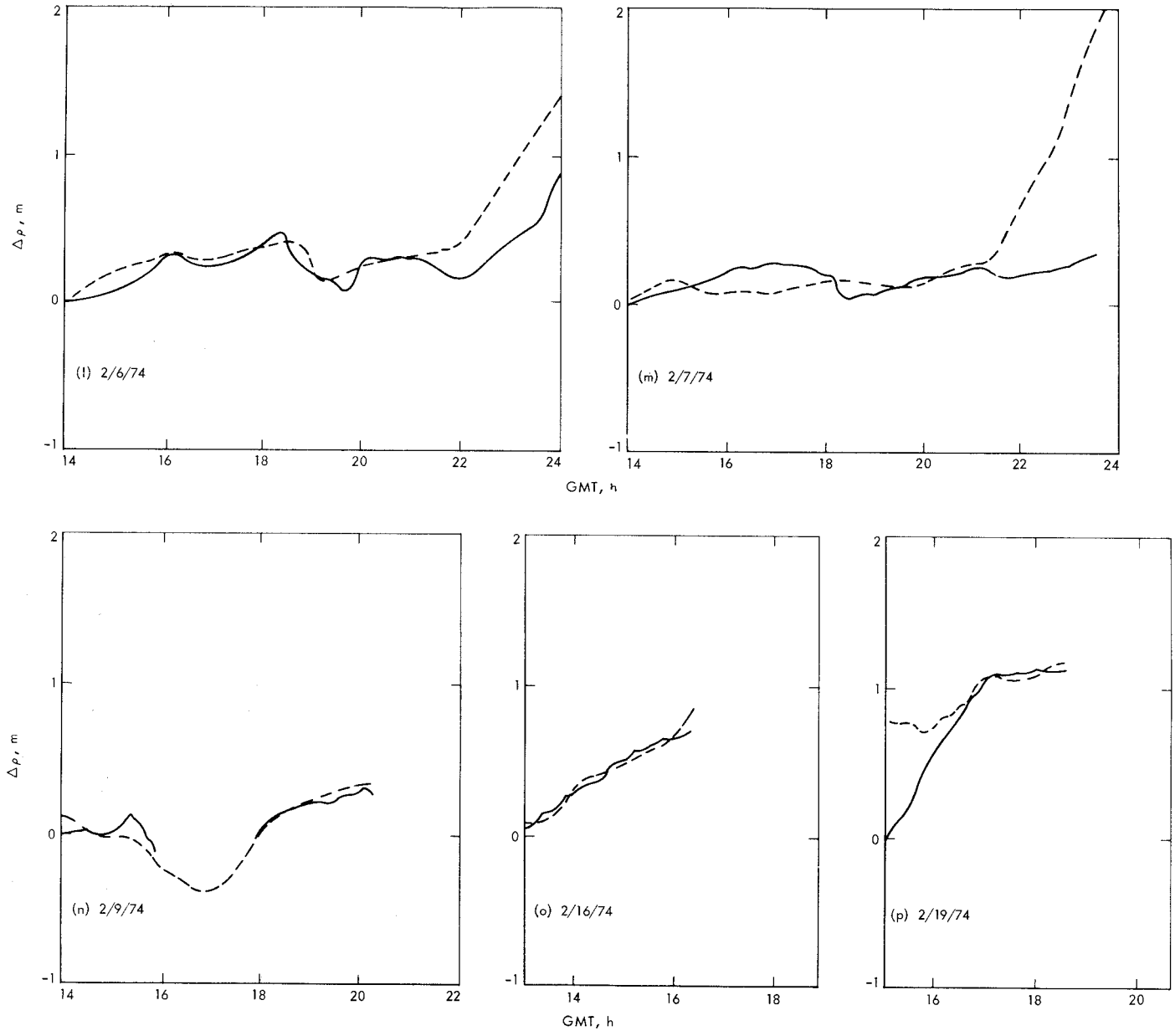

Fig. 1 (contd)

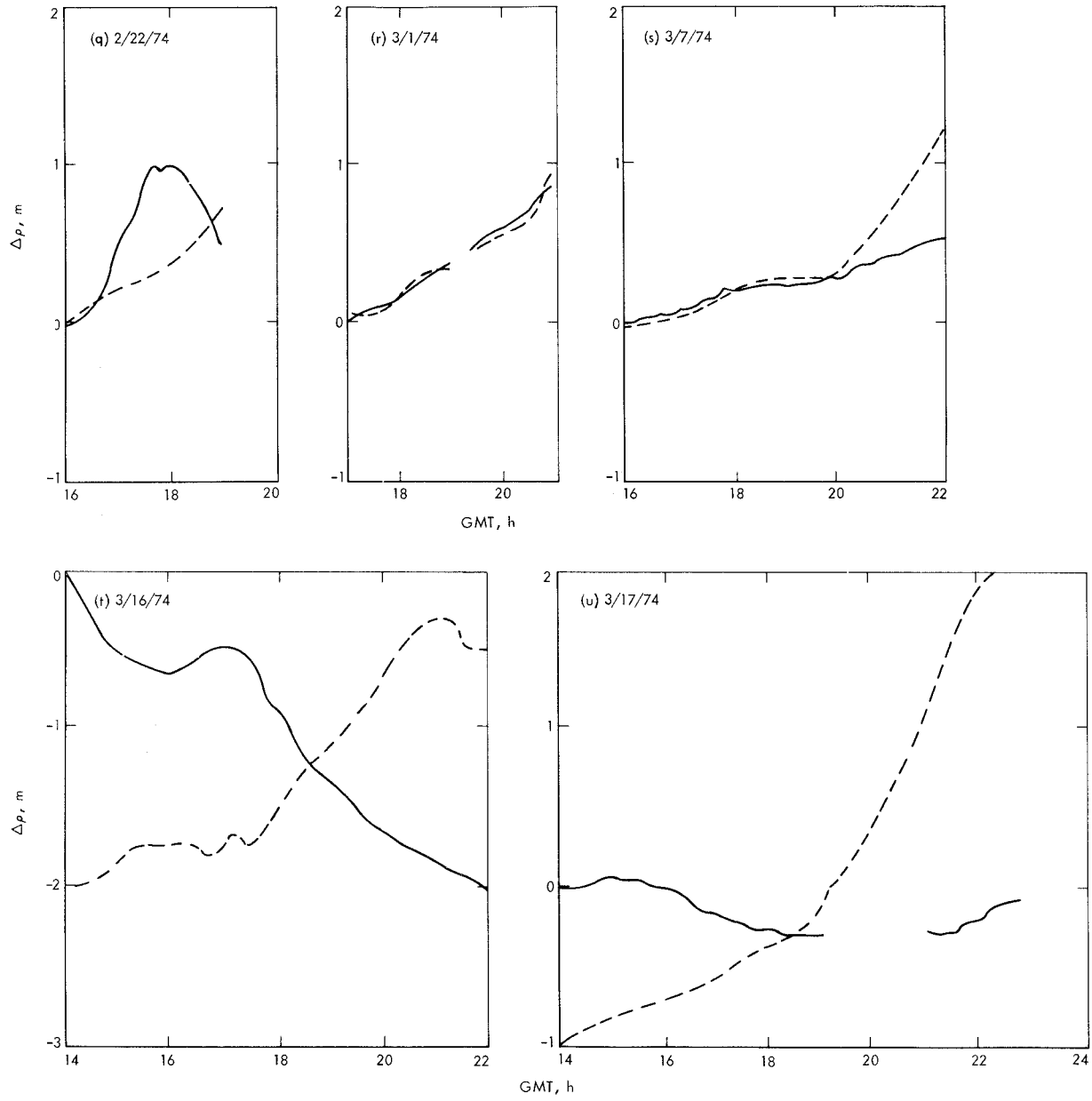

Fig. 1 (contd)

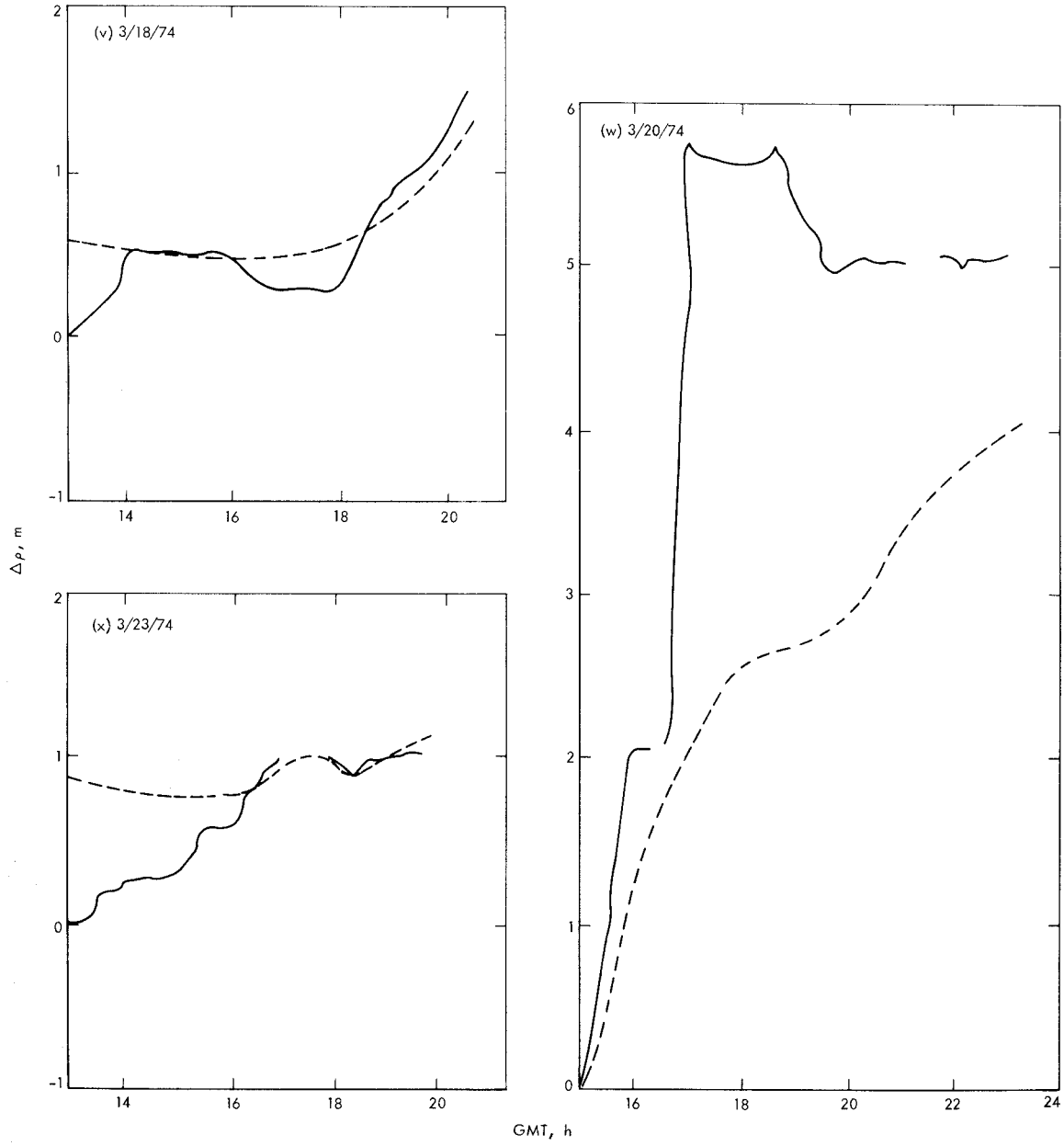

Fig. 1 (contd)

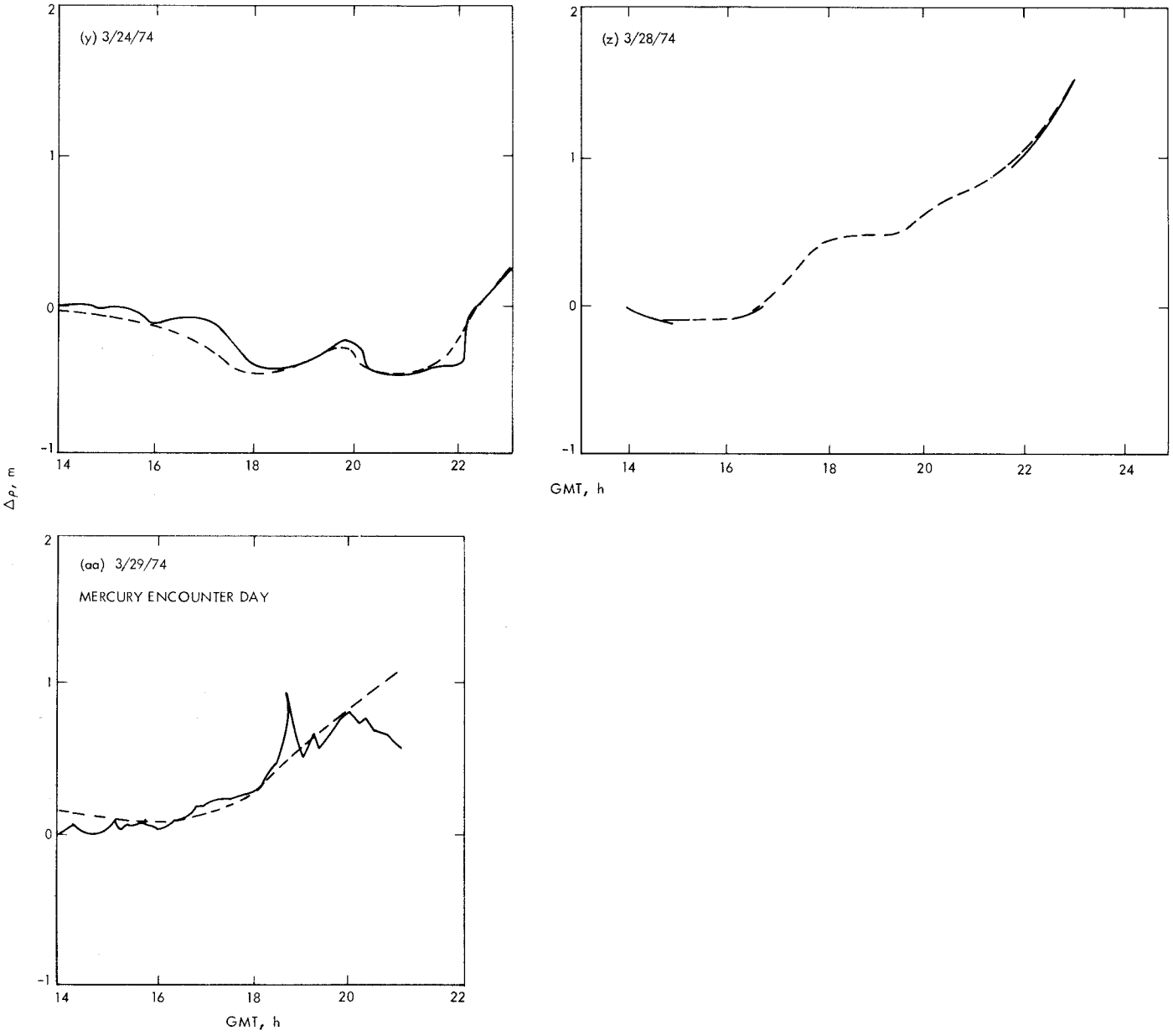

Fig. 1 (contd)

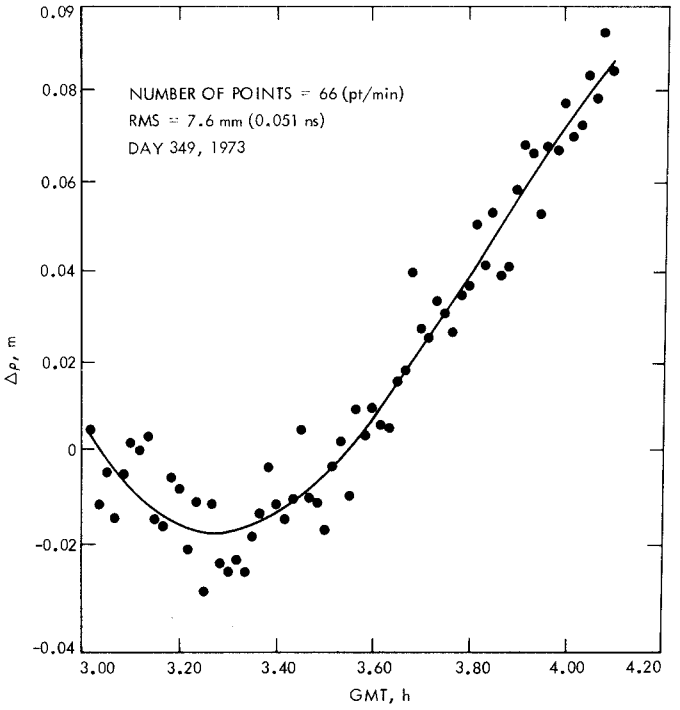

Fig. 2. High-frequency S/X dual doppler noise

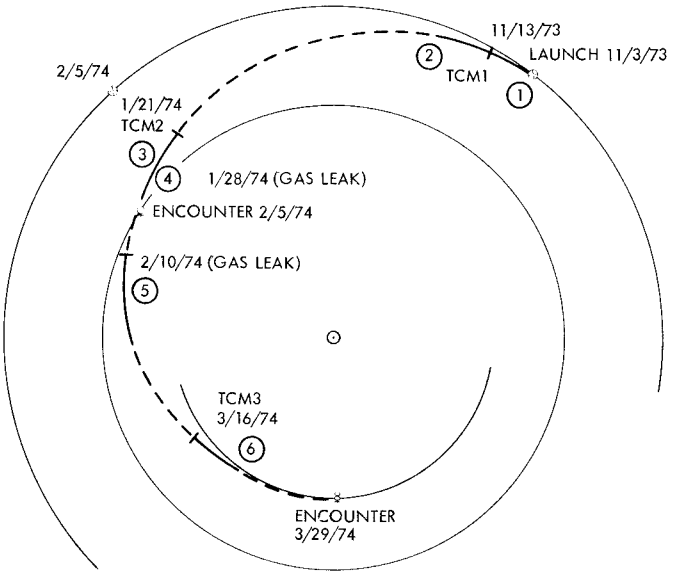

TRAJECTORY ARC 1: CALIBRATED FOR CHARGED PARTICLES VIA FARADAY AND DRVID (REFS. 2-6)

TRAJECTORY ARC 2: CALIBRATED FOR CHARGED PARTICLES VIA FARADAY (REF 3)

TRAJECTORY ARC 3: CALIBRATED FOR CHARGED PARTICLES VIA FARADAY (REF 4)

TRAJECTORY ARC 5: CALIBRATED FOR CHARGED PARTICLES VIA FARADAY

TRAJECTORY ARC 6: CALIBRATED FOR CHARGED PARTICLES VIA FARADAY AND S/X DUAL DOPPLER (REF 5)

Fig. 3. Trajectory segments: short data arcs calibrated and reduced

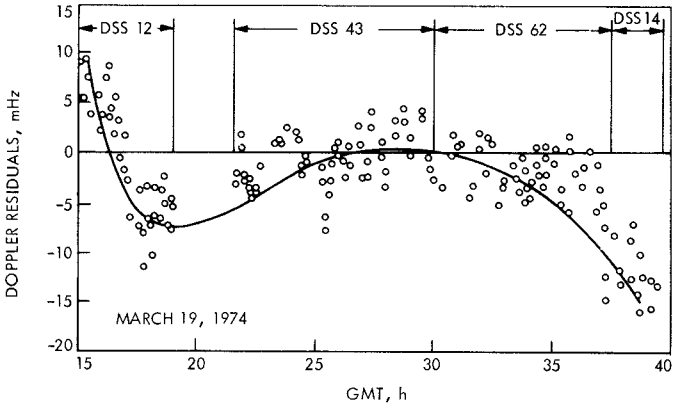

Fig. 4. Space plasma signature present in doppler residuals (count time = 600 s)

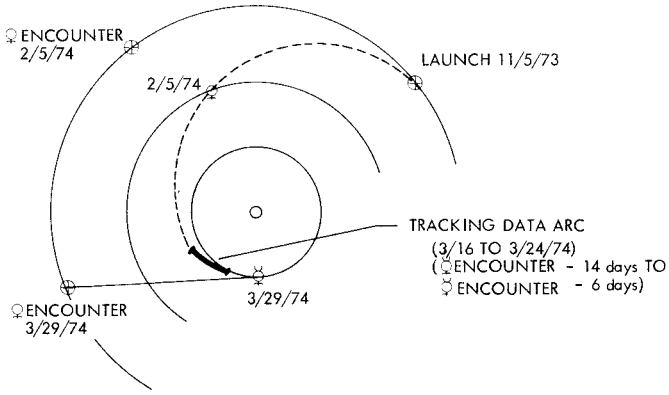

Fig. 5a. Heliocentric plot: MVM'73 transfer trajectory with short data arc shown

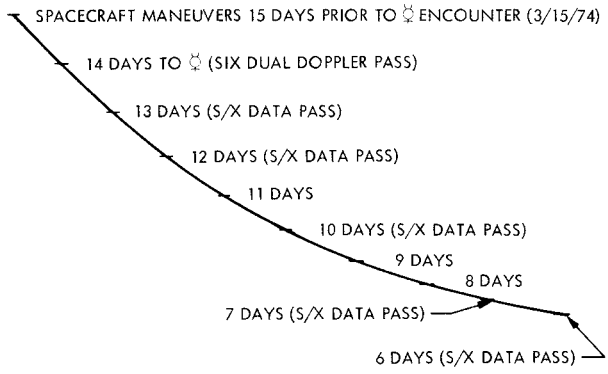

Fig. 5b. S/X dual doppler distribution over tracking data arc

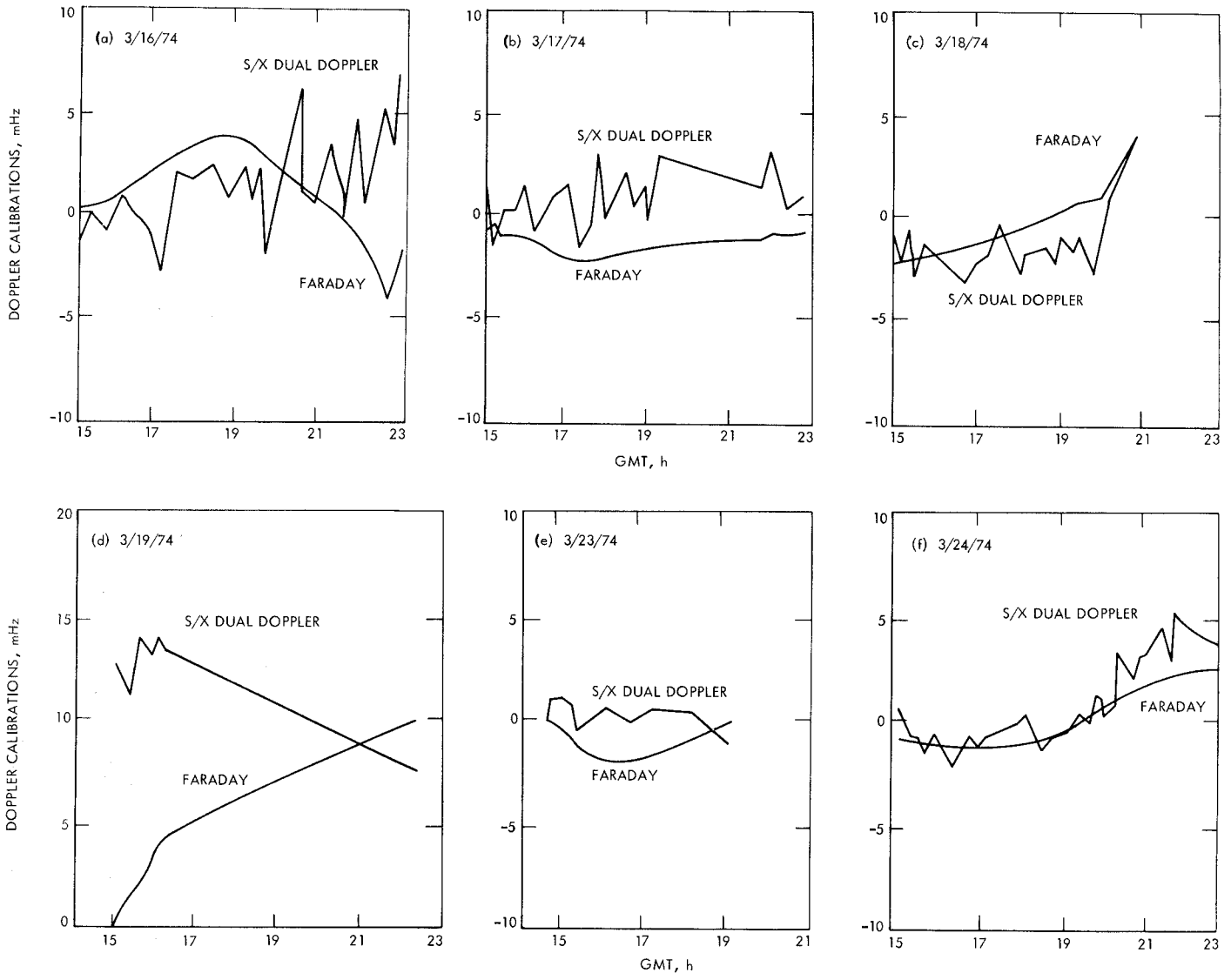

Fig. 6. Doppler calibrations: S/X dual doppler and Faraday polarization

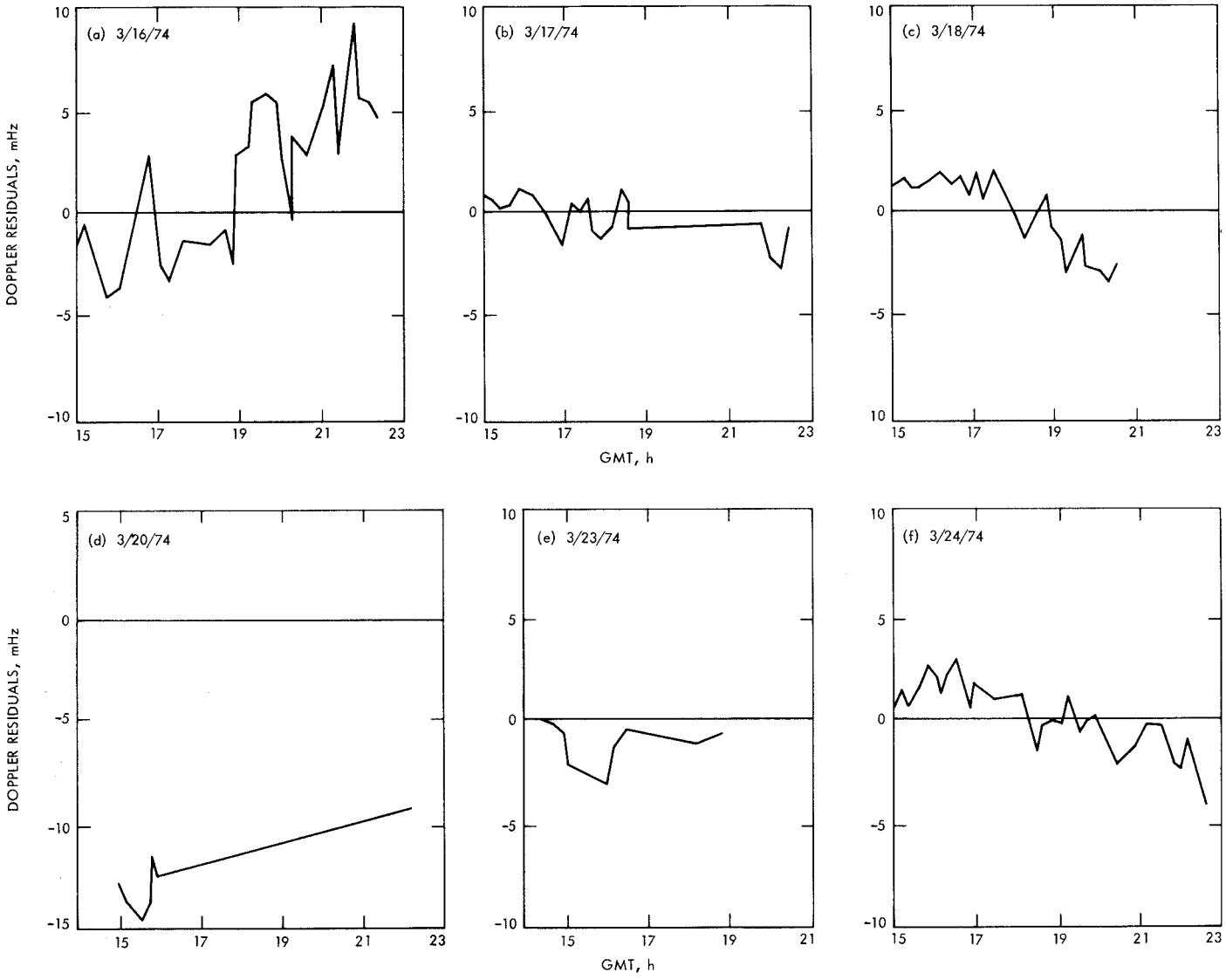

Fig. 7. S-band doppler residuals (600-s count time; no charged-particle calibrations)

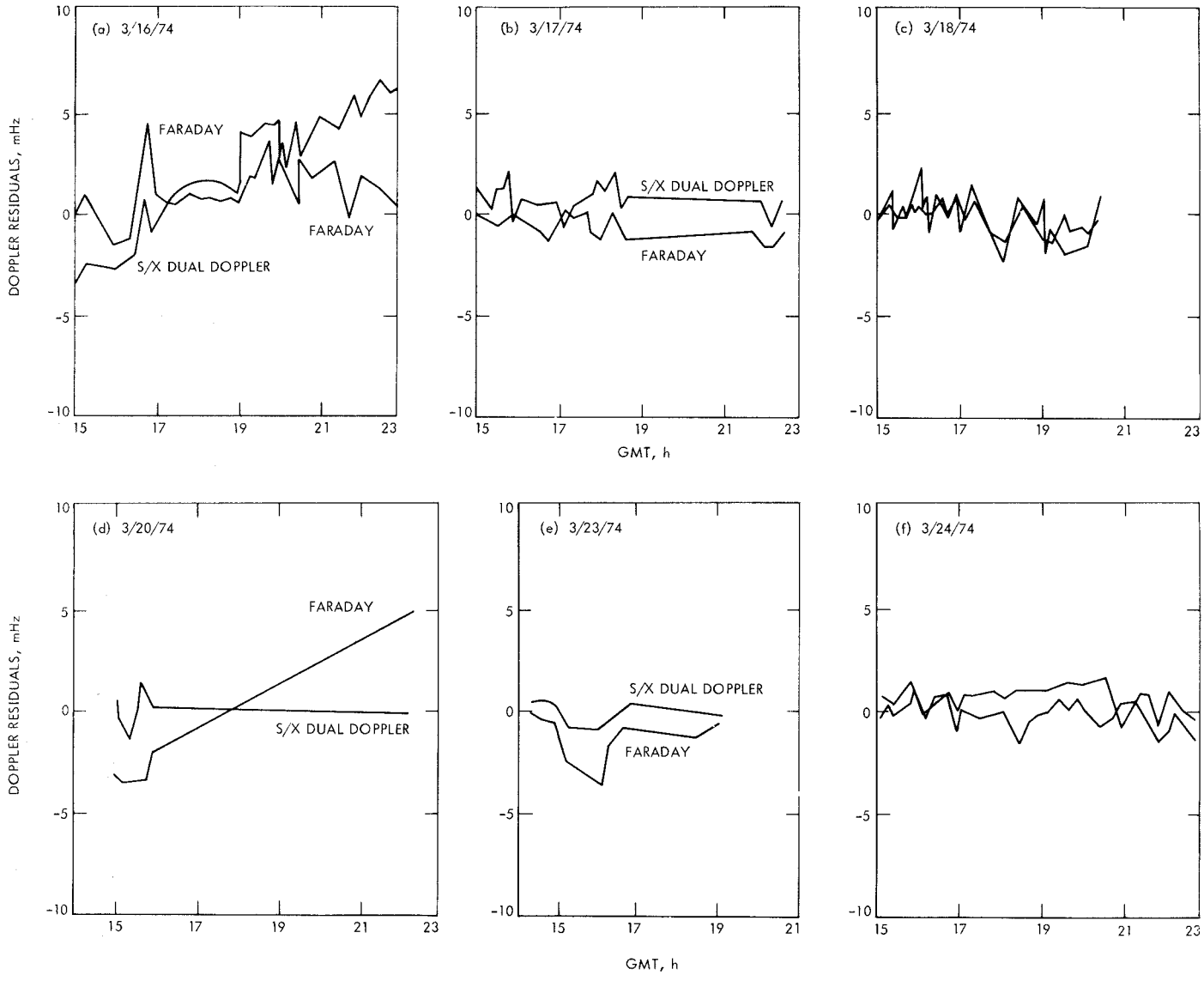

Fig. 8. Doppler residuals: calibrated for charged-particle influences

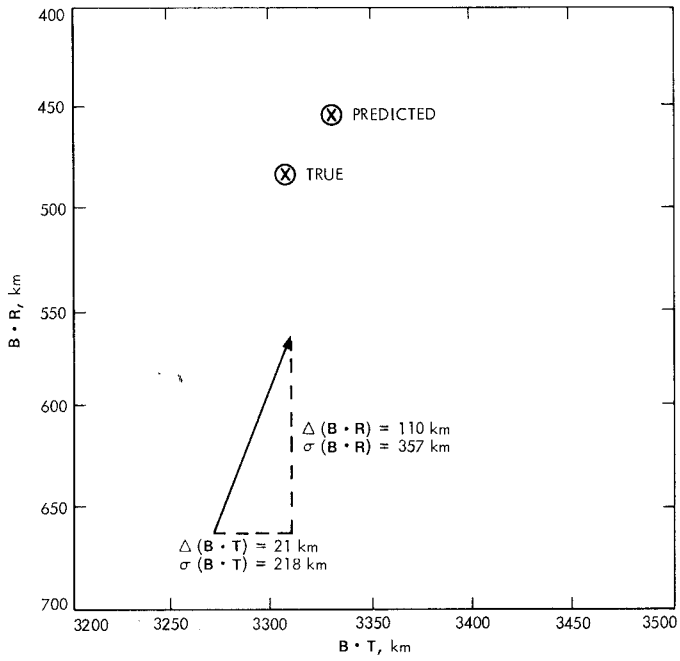

Fig. 9. MVM'73 Mercury encounter plane coordinate estimates: Impact of Faraday calibrations

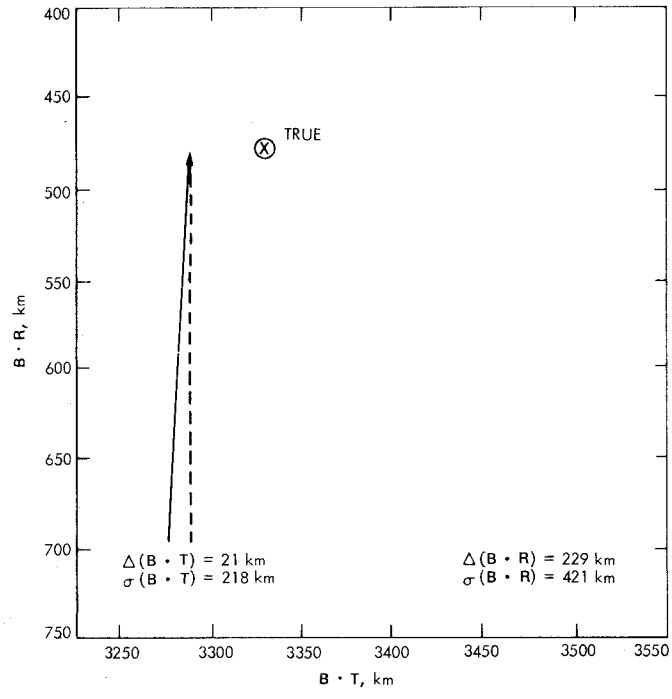

Fig. 11. MVM'73 Mercury encounter plane coordinate estimates: Impact of charged-particle calibrations

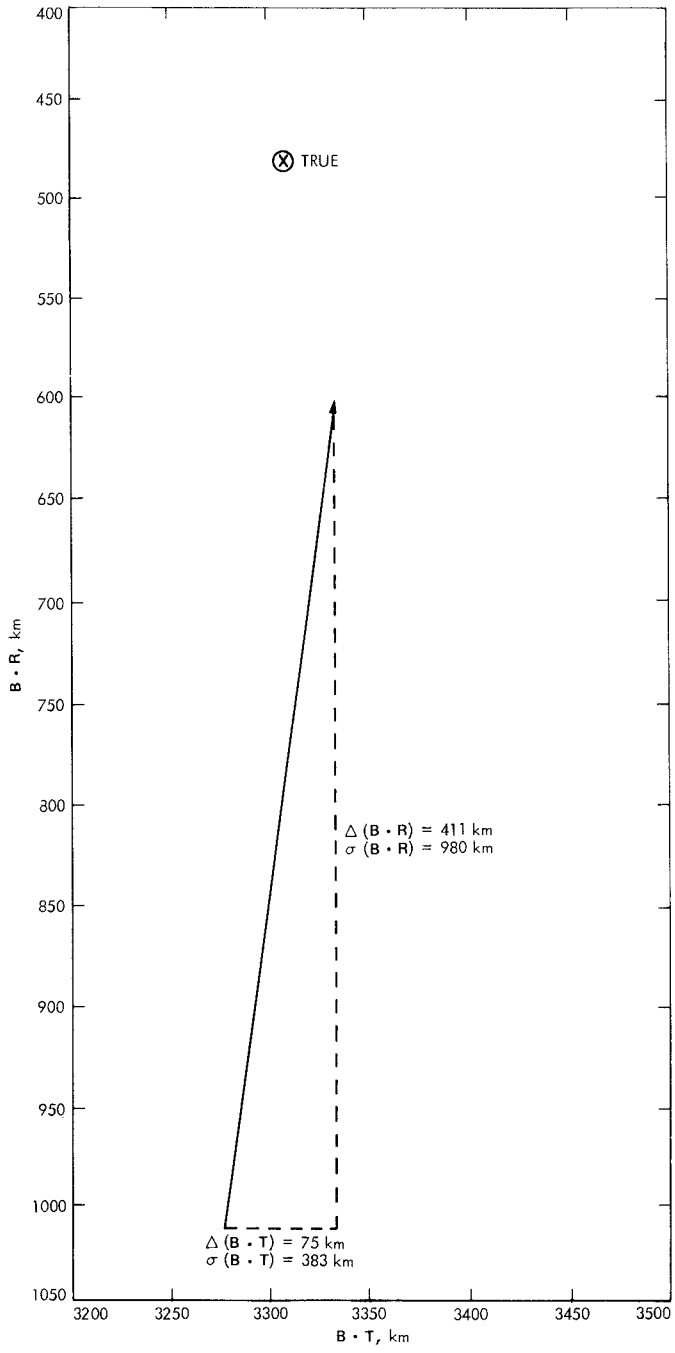

Fig. 10. MVM'73 Mercury encounter plane coordinate estimates: Impact of S/X dual doppler calibrations

Appendix

Verification of S/X Dual Doppler Charged-Particle Calibrations

I. Introduction

S/X dual doppler is demonstrated to provide reasonable charged-particle measurements. This statement is based on the comparisons of three S/X dual doppler and Faraday rotation data passes. Thus, the S/X data quality can only be validated to the accuracy of the Faraday charged-particle computations. The accuracy limitation of the Faraday charged-particle evaluations is discussed.

II. S/X Pass 1: Day 349, 1973

The first S/X data of suitable quality were obtained at DSS 14 on December 15, 1973 (Fig. A-1). The data spans ~6 h. They reveal a long-term decrease in the line-of-sight electron content: a 1-m decrease over the 6-h interval. In addition to the long-term signature, there is also a repetitive short-term structure (~40 min from one local maximum to the next). These short-term structures have been found to be correlated with the roll limit cycle of the spacecraft by B. W. Dysart and W. Martin. Modifications of the DSS 14 experimental dual-frequency receivers corrected this problem. Subsequent S/X data passes do not show this repetitive structure.

The Faraday rotation data (Fig. A-2) only assess the variation of the electron content of the Earth's ionosphere, while the S/X dual doppler data assess the variation of the electron content of the ionosphere and the space plasma collectively. Since the S/X and Faraday data yield electron contents that do not drift relative to each other by more than 0.2 m, the plasma must not exceed this level during this 6-h period.

Earth's ionosphere is being monitored by means of Faraday rotation measurements to the geostationary satellite ATS-1 from DSS 13. However, this only gives the total electron content along this line of sight. These columns of electron content are then projected to the zenith at the ionospheric reference point (the point where this line of sight pierces the ionosphere at 350 km, longitude = 239.5 deg, latitude = 32.6 deg) before they are time-translated to the MVM'73–DSS 14 line of sight (Fig. A-3). The Z's in the Faraday rotation plots (Fig. A-4) represent the time-translated zenith columns. These are then mapped to the respective elevation angles of the station–spacecraft line of sight in the view period by means of a ray trace technique based on a Chapman ionospheric model (Ref. 1). These are the R's in the Faraday plots. As will be seen later, this mapping technique is relatively accurate for elevation angles > 30 deg (Ref. 1). As expected, the Chapman model fails when dawn, dusk, and nighttime ionospheric regions are involved, i.e., the model fails when the solar zenith angle, X, exceeds 80 deg ($-80° < X < 80°$) (Ref. 9).

The latitude and longitude variations of the subionospheric reference points of the DSS 14–MVM'73 and the DSS 13–ATS-1 lines of sight (Fig. A-3) are ~1 deg apart at 24 h UT. This separation is ~100 km in the ionosphere (at reference height of 350 km). If this geometry were the only consideration, the S/X and Faraday data would be matched in range at 24 h UT, by adding a bias to the S/X data. However, there is a second consideration. The DSS 13–ATS-1 data are mapped to the "reference zenith" as previously stated. To be consistent with the total zenith electron contents of other ionospheric observatories, this "mapping in elevation" is accomplished by simply multiplying the acquired data by the cosine of the elevation angle at the subionospheric reference point. The zenith electron content is then mapped to respective elevation angles as mentioned. The error in the first mapping is ~1%. The error in the second mapping is ~5% for elevation angles >30 deg and 20% for angles between 15 and 30 deg. Consequently, the S/X and Faraday data are to be matched in range midway between the time of "closest approach" and "meridian crossing."

A pictorial of the ionospheric and the DSS 14 (December 15, 1973) tracking data acquisition pattern (Fig. A-5) shows the DSS–probe line of sight to pass through the "active region" of the ionosphere for most of the tracking pass. The maximum electron content encountered during this tracking period is encountered just after spacecraft rise and the least electron content encountered at spacecraft set. As a consequence, the ionosphere most influences the doppler data early in the pass, and its influence diminishes as the pass progresses.

The elevation angle is lowest early in the tracking pass (Fig. A-2); thus, at the time when the electron content is largest, the radio signal traverses more ionosphere. As the pass proceeds, the amount of ionosphere traversed decreases.

A comparison of the Faraday rotation and S/X evaluations of the electron content history over the pass reveals the long-term trends to match (Fig. A-2). The maximum disagreement is ~0.15 m at 23 h 51 min. This is ~10% of the total correction at that time. The short-term variations of the Faraday and S/X evaluations do not correlate.

Short-term variations of the ionospheric electron content with amplitudes less than tenths of meters are usually localized (10 to 100 km, Ref. 10). Hence, fine structure variations along the DSS 14–MVM'73 line of sight can not be obtained by mapping the fine structure variations from the DSS 13–ATS-1 line of sight. The short-term variations (Fig. A-2) of the Faraday and S/X data do not correlate and the maximum difference is <0.2 m. From the differences pictured in Fig. A-2, it can be deduced that the localized, short-term, ionospheric variations are ~0.25 m/h (~3×10^{16} electrons/m^2/h). This is quite reasonable.

III. Pass 2: Day 364, 1973

The seven hours of S/X doppler data for Day 364 (December 30, 1973) is similarly compared with the Faraday rotation data and plotted in Fig. A-6. Again, the agreement of the gross trends is good. In this pass, however, the agreement of the S/X and Faraday data at the beginning and the end of the pass is only at the 0.2–0.3-m level. Although the elevation angle of the spacecraft is quite high (~40 deg) in the beginning of the pass, the separation of the DSS 14–MVM'73 and DSS 13–ATS-1 lines of sight is more than 5 deg (~600 km). Moreover, transient electron content irregularities along either line of sight can amount to 0.2–0.3 m. Towards the end of the pass where the elevation angle to the spacecraft dropped to less than 30 deg, the elevation mapping uncertainty becomes larger. Moreover, calculations show that the solar zenith angle (X) on this day becomes larger than 90 deg at UT $\simeq$ 25 h. It is known that the Chapman profile for the ionospheric electron distribution is valid only for $X \lesssim 80$ deg (Ref. 9). Towards dusk, the free electrons in the ionosphere recombine with the positive ions and the electron distribution may not be well defined. A new model for the ionosphere, which treats the daytime, nighttime, dawn, and dusk regions individually, has been theoretically developed (Ref. 1). The implementation of this new model is still not ready, however. Therefore, it is not possible at the present time even to guess what the actual errors will be, using the Chapman model for these dawn and dusk transition zones. In short, the disagreement towards the end of this pass is probably due to a combination of the uncertainties in the elevation angle mapping technique and in the application of the Chapman ionospheric profile.

IV. Pass 3: Day 003, 1974

The S/X–dual doppler data acquired on Day 003 (January 3, 1974) compare even better with the Faraday measurements (Fig. A-7). This stems from two developments: DSS 14 S/X hardware had been modified, and the data were taken only at the higher elevation angles. The maximum difference between the mapped Faraday and the S/X measurements is <0.05 m.

V. Summary

S/X dispersive doppler from DSS 14 does measure the charged particles along the station–spacecraft line of sight at least to the accuracy of the "mapped" Faraday polarization data (0.1–0.3-m level). This conclusion is based on the analyses of data from three DSS 14 tracking passes.

References

1. Yip, K. W., and Mulhall, B. D., "A System Analysis of Error Sources in the Technique Used for Ionospheric Calibration of Deep Space Probe Radio Metric Data," in *The Deep Space Network Progress Report*, Technical Report 32-1526, Vol. XVII, pp. 48–67, Jet Propulsion Laboratory, Pasadena, Calif., Oct. 15, 1973.

2. MacDoran, P. F., "A First-Principles Derivation of the Differenced Range Versus Integrated Doppler (DRVID) Charged-Particle Calibration Method," in *The Deep Space Network*, Space Programs Summary 37-62, Vol. II, pp. 28–34, Jet Propulsion Laboratory, Pasadena, Calif., Mar. 31, 1970.

References (contd)

3. Winn, F. B., and Trask, D. W., *VK75 Mission B Solar Plasma Sensitivities,* TM 391-437, Apr. 9, 1973 (JPL internal document).

4. Winn, F. B., Yip, K. W., and Dysart, B. W., *Current MVM'73 Charged Particle Calibration Experience (21 November 1973),* IOM 391.3-763, Dec. 5, 1973 (JPL internal document).

5. Winn, F. B., and Yip, K. W., *Ionospheric Charged Particle Influence on Mercury B-Plane Coordinate Estimates (Report 4—March 16 to March 24, 1974),* IOM 391.3-787, Apr. 5, 1974 (JPL internal document).

6. Winn, F. B., and Yip, K. W., *Actual Corruption of the MVM'73 B-Plane Coordinate Estimates: Ionospheric Charged Particle Influences on Goldstone DSN Tracking Data (Report 3—January 21 to February 5, 1974),* IOM 391.3-775, Feb. 22, 1974 (JPL internal document).

7. Winn, F. B., and Yip, K. W., *Actual Corruption of the MVM'73 B-Plane Coordinate Estimates: Ionospheric Charged Particle Influences on Goldstone DSN Tracking Data (Report 2—December 20, 1973),* IOM 391.3-770, Jan. 29, 1974 (JPL internal document).

8. Winn, F. B., and Yip, K. W., *MVM DRVID and Its Use in the Orbit Determination Process,* IOM 391.3-789, Apr. 1974 (JPL internal document).

9. Rishbeth, H., *Introduction to Ionospheric Physics,* Academic Press, New York, 1969.

10. Titheridge, J. E., "Large Scale Irregularities in the Ionosphere," *J. Geophys. Res.,* Vol. 68, p. 3399, 1963.

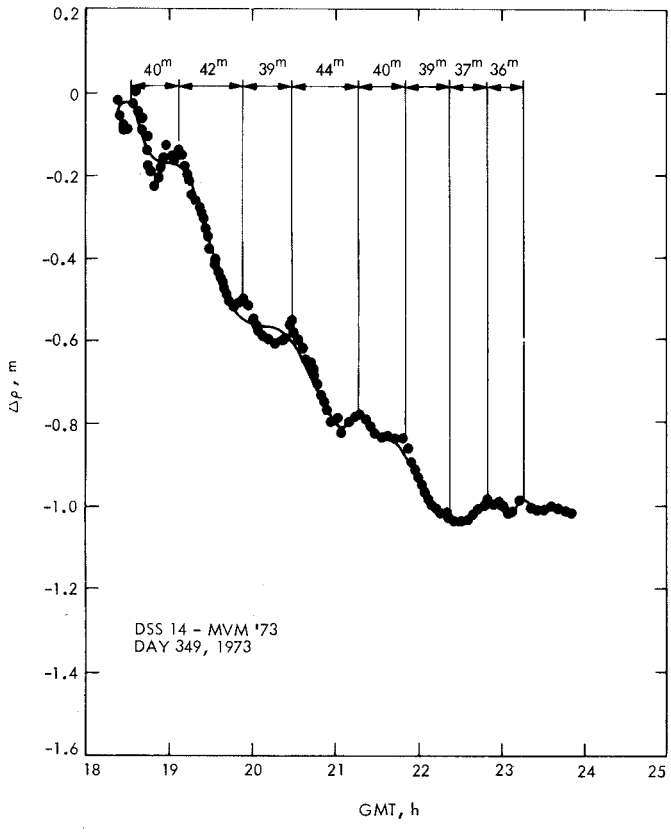

Fig. A-1. S/X dual doppler measurements

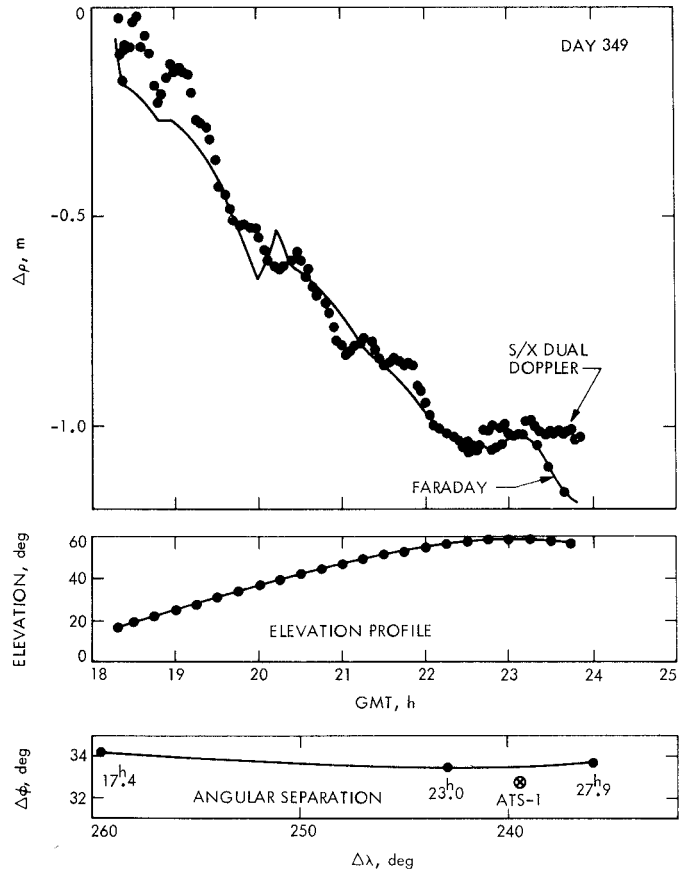

Fig. A-2. S/X dual doppler vs Faraday polarization data

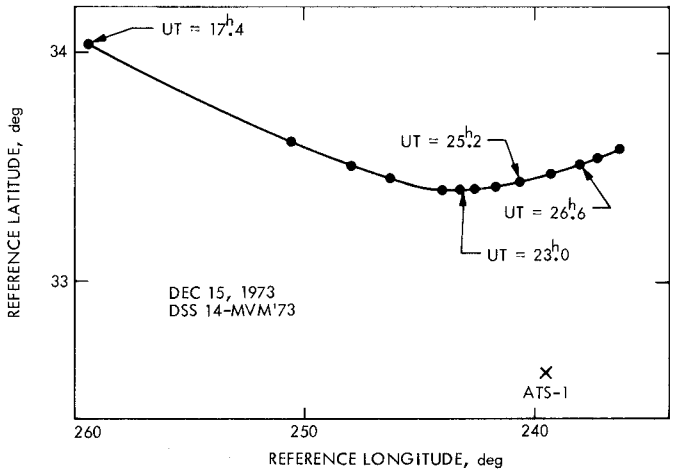

Fig. A-3. Variation of ionospheric reference coordinates

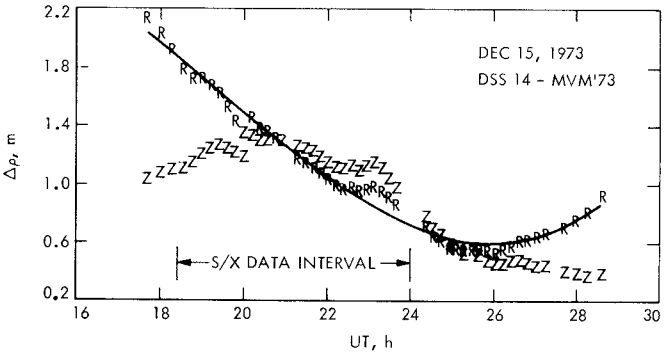

Fig. A-4. Electron content at zenith and along spacecraft line of sight

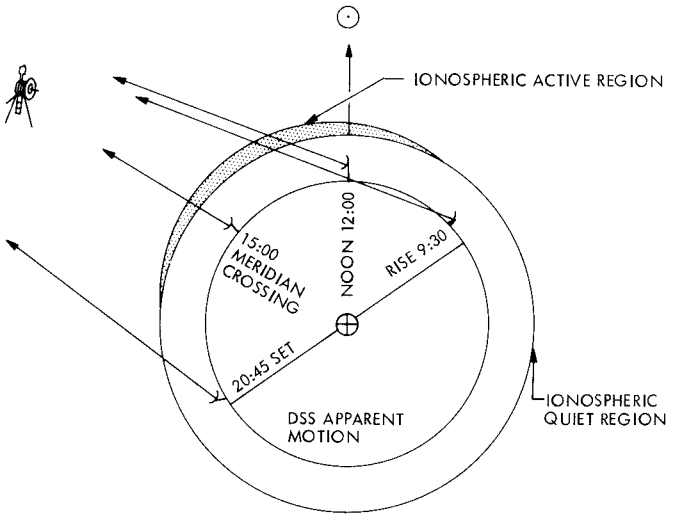

Fig. A-5. Pictorial of the ionosphere involved

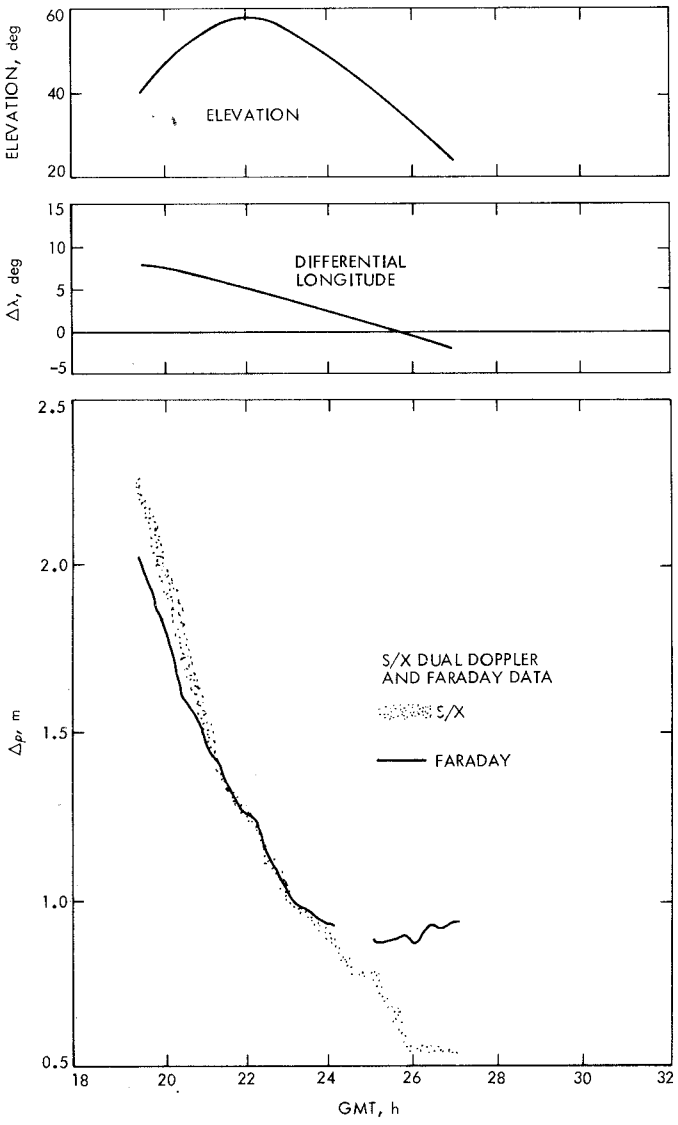

Fig. A-6. S/X pass of Day 364, 1973

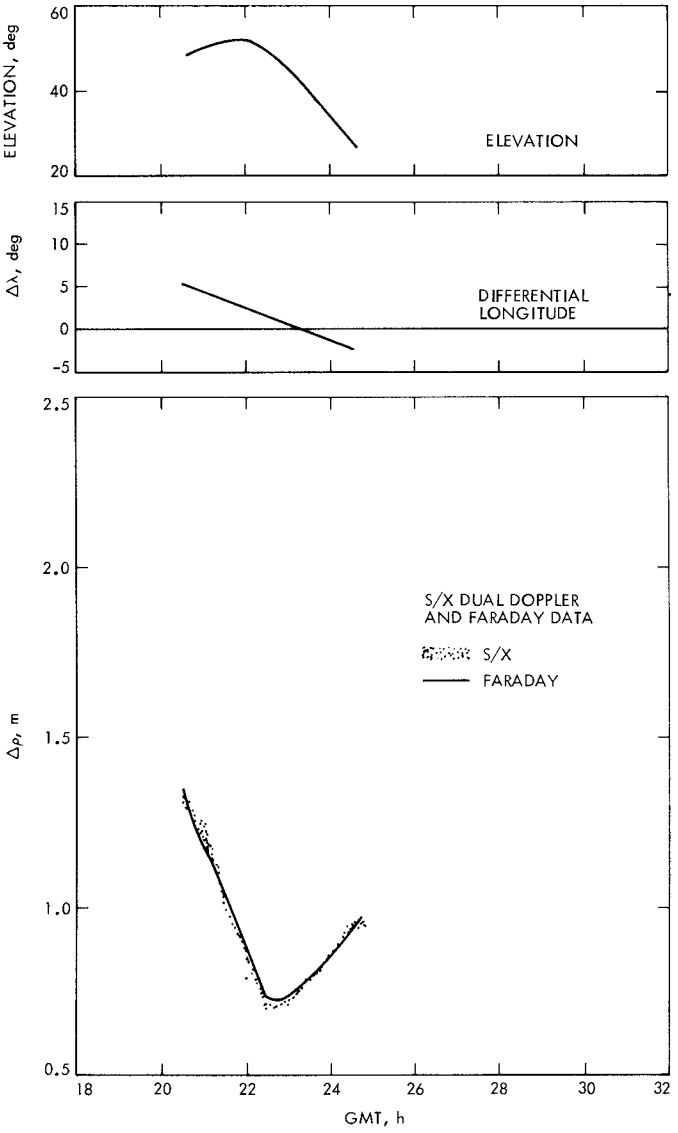

Fig. A-7. S/X pass of Day 003, 1974